Ann Nucl Med
DOI 10.1007/s12149-010-0352-3

ORIGINAL ARTICLE

The reproducibility of deep-inspiration breath-hold ^{18}F-FDG PET/CT technique in diagnosing various cancers affected by respiratory motion

Shigeki Nagamachi · Hideyuki Wakamatsu · Shogo Kiyohara · Seigo Fujita · Shigemi Futami · Hideo Arita · Shozo Tamura · Keiichi Kawai

Received: 7 October 2008 / Accepted: 9 December 2009

Abstract
Background The deep-inspiration breath-hold PET/CT (DIBH PET/CT) technique improves the limitations of diagnosing a lesion located in an area influenced by respiratory motion that results in spatial misregistrations caused by respiration between PET and CT. However, its reproducibility with regard to calculating the maximal standardized uptake value (SUV_{max}) and metabolic volume (MV) in DIBH PET/CT has not been elucidated.
Objective The purpose of this study was to investigate the reproducibility of the DIBH PET/CT technique including calculating the SUV_{max} and the MV.
Methods Sixty patients with various cancers were enrolled. The subjects had 47 abdominal lesions and 28 chest lesions. All patients demonstrated a misregistered image in the early whole-body image taken 50 min after FDG intravenous infusions. We added the delayed spot images 40 min after the first image. On the delayed image, we performed both conventional techniques with non-breath-hold (NBH) and the DIBH technique. In the four times DIBH technique, we obtained the coefficient of variance (CV) in calculating these indices for evaluating reproducibility.
Results The SUV_{max} value with DIBH showed an increase of 16.1–60.1% compared with that measured by NBH. The mean value of CV was 5.5 in thoracic lesions and 6.3 in abdominal lesions. The values of MV with DIBH showed a decrease of 14.0–20.1% compared with those measured by NBH. Regarding reproducibility, mean value of CV was 7.1 in thoracic lesions and 11.9 in abdominal lesions.
Conclusion The DIBH technique improves the inaccurate quantification of both SUV_{max} and MV. Although the CV value of SUV_{max} with DIBH technique is better in thoracic lesions compared with that in abdominal lesions, the reproducibility was acceptable.

Keywords ^{18}F-FDG PET/CT · Deep-inspiration breath-hold · Reproducibility

Introduction

The combined PET/CT imaging yields increased sensitivity and specificity than either of the two modalities and, therefore, provides improved diagnostic accuracy for various cancers [1–4]. Because attenuation correction in PET is performed with the use of CT data, accurate spatial registration of PET and CT image sets is required. In the interpretation of PET/CT imaging, therefore, the misalignment of structures and lesions owing to respiratory motion is a significant problem [5–7]. It causes not only the misdiagnosis of tumor location, but also errors of quantification [6, 8, 9]. To overcome this drawback, respiratory gating of PET and CT is available using specific equipment for gating data acquisition [7, 10–13]. However, the method requires a long acquisition time for processing the examination because we have to divide collection data into certain phases [9–11]. Recently, the deep-inspiration breath-hold (DIBH) technique has been reported to be

S. Nagamachi (✉) · H. Wakamatsu · S. Kiyohara · S. Fujita · S. Futami · H. Arita · S. Tamura
Department of Radiology, School of Medicine, Miyazaki University, 5200 Kihara, Kiyotake, Miyazaki 889-1692, Japan
e-mail: snagama@med.miyazaki-u.ac.jp

K. Kawai
Faculty of Health Science, School of Medicine, Kanazawa University, Ishikawa, Japan

Published online: 11 March 2010

likely to overcome these problems. Particularly, it has been validated as a useful technique in the diagnosis of thoracic lesions, such as lung cancer [14–17].

The effectiveness of DIBH is related to identifying anatomical localizations as well as providing correct quantification. According to a previous report, the maximal standardized uptake value (SUV_{max}) values with DIBH PET were significantly higher than those obtained with conventional non-breath-hold (NBH) PET [14, 15]. Using the deep-inspiration breath-hold PET/CT (DIBH PET/CT) technique, therefore, we can accurately evaluate lesions close to the diaphragm in quantitative analysis. However, to maintain a good quality imaging of DIBH PET/CT, we need to repeat the DIBH technique and add some images. Therefore, if CT images and repeated DIBH PET images do not match constantly and completely, attenuation correction and SUV calculation will be inaccurate. To the best of our knowledge, the reproducibility in the quantification of SUV_{max} or MV by DIBH has not been focused on previously.

The purpose of the current study was to investigate the reproducibility of the deep-inspiration breath-hold ^{18}F-FDG PET/CT (DIBH PET/CT) techniques in quantitative analysis.

Materials and methods

Phantom study

Before clinical research of DIBH, we performed a phantom experiment to examine the coefficient of variance (CV) of ^{18}F-FDG PET indices in imaging of motionless objects. We used a cylinder phantom (10-cm high, diameter of 20 cm, etc. test phantom, Kyoto Kagaku, Japan) and set three elliptical pillar phantoms (8.0-cm high, diameter 2.0 cm, Kyoto Kagaku, Japan) filled with ^{18}F-FDG aqueous solution of different radioactivity (64, 32, and 8 kBq/ml) concentrations in a cylinder phantom. ^{18}F-FDG was provided by Nihon MediPhysics Company (Kurume, Fukuoka prefecture, Japan). All data were acquired on a combined PET/CT in-line system (Biograph 16, Siemens). The PET/CT scan was performed using a single bed position. CT was used for CT-based attenuation correction. PET emission data were acquired using a static collection method for 2 min and for 30 s. In condition with 30 s collections, a total of 4 images were obtained per concentration.

All PET images were reconstructed using iterative algorithms (Fourier rebinning plus attenuation-weighted ordered-subset expectation maximization, 2 iterations, 8 subsets, 5-mm Gaussian filter) with CT-based attenuation correction. The data were reconstructed with a 256 × 256 matrix and 2-mm slice thickness.

Image analysis was performed on a dedicated workstation (ESOFT4.5, Siemens). On the 3-dimensional (coronal, sagittal and axial) PET/CT images, volumes of interest (VOIs) were drawn automatically around each cube above a pre-set threshold of 50% of the maximal value of radioactivity (Bq/ml), and 3-dimensional isocontours at 50% of the maximal value of radioactivity (Bq/ml). We also calculated the metabolic volume (MV) of each cube. We defined the MV as the total areas with radioactivity (Bq/ml) exceeding 50% of the maximal value of radioactivity.

The means and standard deviations (SDs) of the maximal value of radioactivity or MV for the 4 images with 30 s data collections were calculated for all with the three-cylinder phantoms with the various ^{18}F-FDG radioactivity concentrations. In addition, we calculated the CV for these indices of four individual DIBH studies. The coefficient of variance (CV) was defined as SD × 100/mean.

Clinical study

The current study was conducted from October 2007 to July 2008. Sixty patients (34 male, 26 female; average age, 63.5 years; age range, 35–72 years) with a biopsy-proven diagnosis of cancer confirmed by staff pathologists at the School of Medicine, Miyazaki University, were included. All patients were selected according to the findings of a whole-body image, which showed misregistration under NBH.

All analyzed lesions comprised 25 liver tumors including multiple metastasis, 11 bile duct cancers including GB cancer and lymph node metastasis, 11 pancreas cancers, 22 lung cancers, 3 esophageal cancers and 3 chest wall tumors. All lesions were solid tumors diagnosed by X-ray CT and ultrasound (US). All patients were free of diabetes or respiratory dysfunction such as chronic obstructive pulmonary disease (COPD). They had normal respiratory function (percentage of vital capacity (%VC) >80.0%, forced expiratory volume in 1 s (FEV 1.0%) >70.0%). With regard to the tumor maximal diameter, there were no significant differences between thoracic lesions and abdominal lesions (Table 1).

We used the following protocol. Patients fasted for at least 5 h before injection of 185 MBq of ^{18}F-FDG. The total ^{18}F-FDG dosage in each person was from 166.5 to 238.5 MBq and the mean dosage was 218.3 MBq (3.76 MBq/kg). During the uptake phase of approximately 50 min, the patients remained in a quiet position. The first whole-body image was obtained in a supine position. The imaging time was 15–18 min for each patient. The acquisition time per bed position was 2 min. In addition to the conventional whole-body PET/CT examination, we added NBH imaging of a spot view. The acquisition time was also

Table 1 Patient's clinical characteristics

	Thoracic lesions ($n = 28$)	Abdominal lesions ($n = 32$)
Age	65.9 ± 10.1	61.3 ± 10.2
Gender (M:F)	16:12	18:14
Respiratory function		
%FEV1	86.3 ± 12.5	87.2 ± 8.9
%VC	91.7 ± 8.9	85.1 ± 8.2
COPD	None	None
Diabetes mellitus	None	None

%FEV1 forced expiratory volume in 1 s
%VC %vital capacity
COPD chronic obstructive pulmonary disease

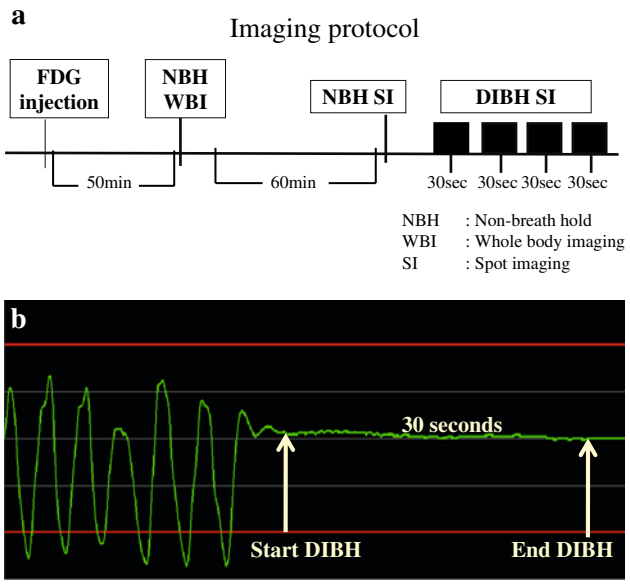

Fig. 1 **a** Protocols for FDG PET/CT imaging of NBH and DIBH. **b** Breathing signal of patient during NBH condition and DIBH PET/CT. Patient was instructed to hold breath in maximal inspiratory position for 30 s during DIBH PET scan

2 min. Just after the NBH imaging, we performed DIBH spot imaging four times in all of the selected patients (Fig. 1a).

Each DIBH image datum was acquired under a condition with 30 s breath holding. The time from the beginning to the end of DIBH condition was recorded by referring to the real-time display of the respiratory monitoring equipment (AZ-733V; Anzai Medical Co. Ltd., Japan). A respiratory sensor (an elasticized belt around the patient's abdomen) provides respiratory information by detecting changes in the patient's abdominal pressure. Before performing the actual DIBH PET/CT examination, the patients repeated exercises of DIBH several times to maintain each DIBH posture equally. During the actual PET scan, patients were asked to hold their breath in maximal inspiratory position motionlessly for 30 s, with the respiratory monitoring device fixed. We confirmed that they were equal to the BH condition by referring to records of the respiratory monitoring system (Fig. 1b).

We used the same clinical reconstruction parameters for both the NBH PET and DIBH PET images. All PET images were reconstructed using iterative algorithms (Fourier rebinning plus attenuation-weighted ordered-subset expectation maximization, 2 iterations, 8 subsets, 5-mm Gaussian filter) with CT-based attenuation correction. The data were reconstructed with a 256 × 256 matrix and 2-mm slice thickness. All PET and CT images were transformed to a dedicated workstation (e-soft; Siemens), from which fusion PET/CT images were constructed.

All patients provided written informed consent. The review board of the Miyazaki University School of Medicine approved this study protocol.

Image analysis

Image analysis was performed on the same dedicated workstation (ESOFT4.5, Siemens) as used for the phantom study, which can display three orthogonal planes for CT, PET and PET/CT fused images and maximum-intensity projection (MIP) images. NBH PET/CT and four kinds of DIBH PET/CT image were visually assessed for the anatomical location of the lesion, and accuracy of fusion and alignment in separate instances by the same nuclear medicine physicians.

On the 3-dimensional (coronal, sagittal and axial) PET/CT images, a VOI of a lesion above a pre-set threshold of 50% of SUV_{max} was automatically drawn using 3-dimensional isocontours at 50% of the maximum SUV. The maximum value in the VOI was defined as SUV_{max}. SUV_{max} was obtained for all lesions revealed on NBH PET/CT images and DIBH PET/CT images.

Both the values of SUV_{max} and MV were compared between NBH images and the mean of four DIBH images. Continuous variables were expressed as mean ± SD. Statistical analyses were conducted by the unpaired Student's *t* test and paired *t* test. A p value of <0.05 was considered to be statistically significant. In addition, we evaluated the reproducibility of calculating these two indices in four DIBH images. Namely, we calculated the CV for both SUV_{max} and MV of four individual DIBH studies. The CV was defined as SD × 100/mean. Then we compared the

mean value of CV in imaging of thoracic lesions with that of abdominal lesions.

Results

The results of the phantom study are shown in Table 2 and Fig. 2. When we calculated the quantitative indices (maximal value of radioactivity and MV) in each of the four 30-s studies, the reproducibility was acceptable in the three kinds of concentrations (Fig. 2). The value of CV in low-dose concentration (8 kBq/ml) was 5.7 and those in the middle-dose (32 kBq/ml) or high-dose concentrations (64 kBq/ml) were 1.2 and 1.1. Regard as CV for calculating MV, the value of CV in low-dose concentration was 12.2 and those in the middle-dose or high-dose concentrations were 3.1 and 2.3, respectively (Table 2).

In the clinical studies, all patients who participated in this current study were able to accomplish this protocol. With regard to the clinical parameters, there were no apparent differences between abdominal lesions and thoracic lesions (Table 1). In both NBH and DIBH images, all lesions were clearly visualized. Under DIBH conditions, all misregistration uptakes were corrected to the normal anatomical location (Figs. 3, 4, 5, 6). The DIBH PET/CT not only allowed a more precise localization of lesions, but also accurately corrected the misregistration under NBH conditions in all cases.

In the quantitative analysis, the mean value of SUV_{max} was statistically higher in the DIBH PET/CT technique than in the NBH study in all evaluated lesions. With regard to the MV, the mean value of each MV was statistically lower in the DIBH PET/CT technique than in the NBH study (Table 3).

The mean value of CV in SUV_{max} was 5.5 in thoracic lesions and 6.3 in abdominal lesions. These values were higher in comparison with those obtained from the phantom experiment with middle- or high-dose concentrations. In the comparison of CV in SUV_{max}, the mean value of CV in thoracic lesions was better than that in abdominal lesions. However, there was no statistical significance. With regard to CV in MV, it was 7.1 in thoracic lesions and 11.9 in abdominal lesions. This difference was not statistically significant either.

Table 2 Comparison of quantitative indices (phantom study)

Parameter	Low dose	Middle dose	High dose
SUV_{max} (Bq/ml)—30 s collection			
1st	3.7 (2934.1)	14.6 (12040.2)	28.2 (23278.4)
2nd	3.8 (3055.2)	14.8 (12013.2)	28.1 (23728.6)
3rd	3.3 (2710.7)	14.5 (11734.4)	27.6 (23268.8)
4th	3.4 (2744.5)	14.8 (11989.2)	27.7 (23177.3)
Mean	3.5 (2861.1)	14.7 (11944.3)	27.9 (23363.3)
SD	0.2 (162.5)	0.17 (141.4)	0.31 (247.8)
CV	5.7	1.2	1.1
SUV_{max} (Bq/ml)—2 min collection			
	3.5 (2801.1)	14.3 (11624.3)	27.4 (23151.9)
MV—30 s collection			
1st	4.4	29.8	62.3
2nd	3.5	27.8	59.1
3rd	4.4	28.2	60.0
4th	4.7	28.8	60.2
Mean	4.2	28.6	60.4
SD	0.5	0.9	1.4
CV	12.2	3.1	2.3
MV—2 min collection			
	4.5	29.3	60.7

SUV_{max} (Bq/ml) maximal standardized uptake value (maximal value of radioactivity count)

MV metabolic volume (ml)

Low dose 8.0 kBq/ml

Middle dose 32.0 kBq/ml

High dose 64.0 kBq/ml

Discussion

Because of its effectiveness, the DIBH technique is usually applied to thoracic lesions [14–17]. It is effective in

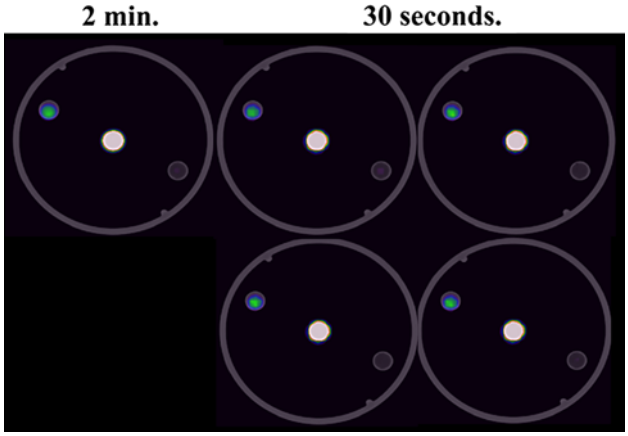

Fig. 2 Results of phantom study. In 2-min collections (*left upper*), the values of SUV_{max} were 3.5, 14.3 and 27.4 (low dose, middle dose, high dose), and MV (ml) were 4.5, 29.3 and 60.7, respectively. In the 30-s collections (*middle* and *right*), each value of SUV_{max} of low dose was 3.7, 3.8, 3.3 and 3.4, respectively. Similarly, each SUV_{max} of middle dose was 14.6, 14.8, 14.5 and 14.8. Each SUV_{max} of high dose was 28.2, 28.1, 27.6 and 27.7. The CV of each concentration was 5.7, 1.2 and 1.1, respectively. Regarding MV (ml) in the 30-s collections, each value of low dose was 4.4, 3.5, 4.4 and 4.7, respectively. The MV (ml) of middle dose was 29.8, 27.8, 28.2 and 28.8. The MV (ml) of high dose was 62.3, 59.1, 60.0 and 60.2. The CV of each concentration was 12.2, 3.1 and 2.3, respectively

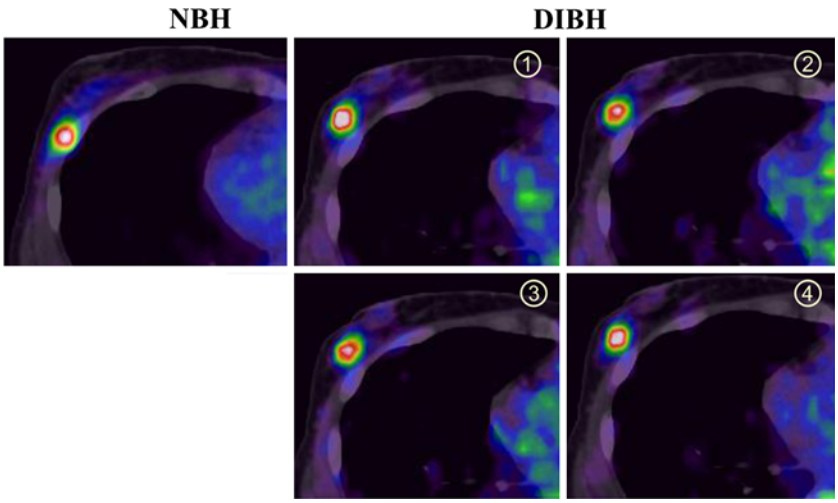

Fig. 3 A 45-year-old woman with right breast cancer. In the NBH image, focal FDG uptake is shown within the rib (*left upper*). The value of SUV_{max} is 9.0 and MV (ml) was 4.5 in the NBH image. Using the DIBH technique, FDG uptake was noted to be consistent with breast cancer. Each value of SUV_{max} was 9.9, 9.3, 9.3 and 9.6, respectively. The value of CV was 3.3. Regarding MV (ml), the values were 4.4, 3.9, 4.4 and 4.2, respectively, and the value of CV was 6.2 (*middle* and *right*)

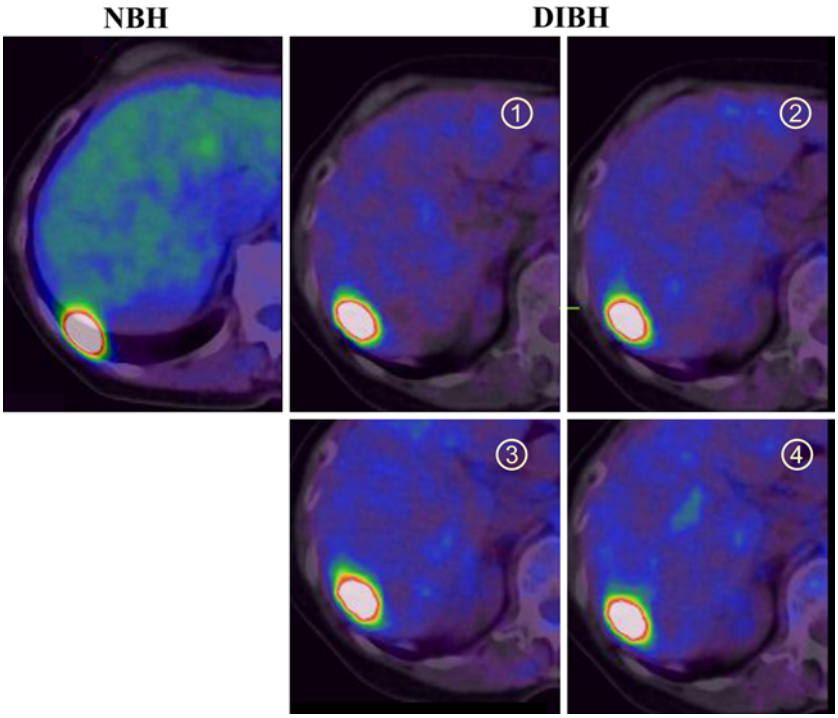

Fig. 4 A 54-year-old woman with liver metastasis from breast cancer. In the NBH image (*left upper*), focal FDG uptake appears to be lung metastasis. The value of SUV_{max} was 16.5 and MV (ml) was 19.5 in NBH. Using the DIBH technique, liver metastasis was correctly recognized. Each value of SUV_{max} in DIBH was 28.5, 29.6, 28.6 and 28.3, respectively. The value of CV was 2.2. Regarding MV (ml) in DIBH technique, the values were 14.4, 14.9, 14.1 and 15.8, respectively, and the value of CV was 5.2 (*middle* and *right*)

diagnosing the exact location of the lesion and evaluation of the number of lesions by avoiding respiratory artifacts. In addition, the method also has the advantage of providing accurate quantitative indices [16, 17].

On the basis of very accurate local coregistration, which makes it possible to perform accurate attenuation correction and also to reduce blurring, increases in SUV_{max} were observed in most cases [14, 16–18]. The SUV_{max} values of DIBH state increased 1.2–1.6 times in comparison with those of the NBH state. This result was comparable to those of previous data with regard to thoracic tumors [10, 16–20]. In this mechanism, the voxel including SUV_{max} is dispersed under the NBH condition with respiratory motion during the entire respiratory cycle, which causes underestimation of the true activity concentration [18–21]. In contrast, under the DIBH condition, the voxel including the SUV_{max} tends to be fixed, resulting in an increase of SUV_{max}. The reason why the effectiveness was prominently noted in thoracic lesions was probably due to the distances moved by respiratory motions. Because thoracic lesions were likely to be more influenced under respiratory motion, SUV_{max} of thoracic lesion demonstrated more remarkable changes than that of abdominal lesions.

The value of MV in the DIBH technique decreased to about 80% of that in NBH in both thoracic and abdominal lesions. In a previous respiration-gated study, a reduction

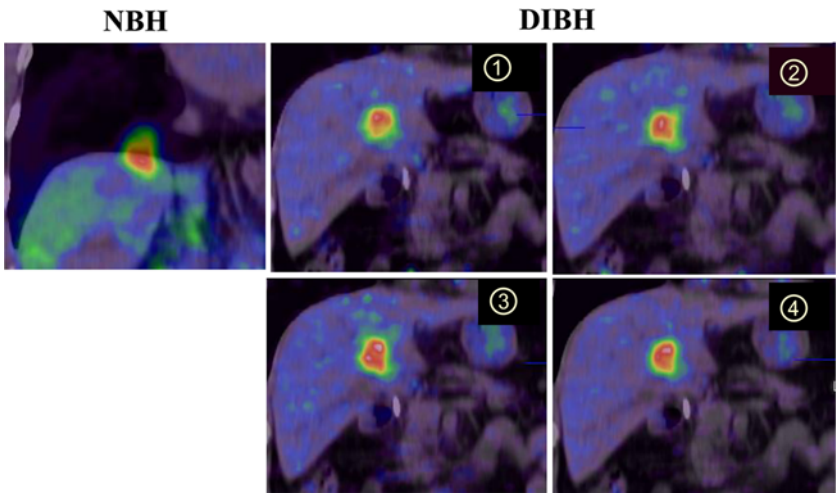

Fig. 5 A 67-year-old man with cholangiocarcinoma. With NBH image, the tumor was identified partly in the chest. The value of SUV_{max} was 8.5 and MV (ml) was 26.8 (*upper left*). Under DIBH condition, the tumor was correctly coregistered. Each value of SUV_{max} was 14.6, 17.2, 16.5 and 16.2, respectively. The value of CV was 6.7. The values of MV (ml) in each DIBH image were 20.3, 20.6, 26.0 and 30.5, respectively, and the value of CV was 19.6 (*middle* and *right*)

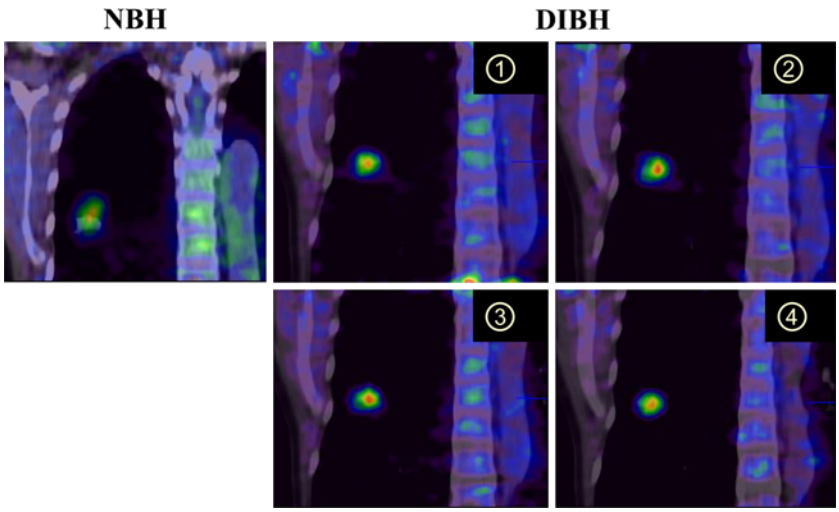

Fig. 6 A 64-year-old man with primary lung adenocarcinoma. With NBH, FDG uptake was partly dissociated with tumor contour. The value of SUV_{max} was 3.2 and MV (ml) was 4.6 (*left upper*). Under DIBH condition, the tumor was correctly coregistered. Each value of SUV_{max} was 6.4, 6.8, 7.0 and 6.5, respectively. The values of MV (ml) in each DIBH image was 3.2, 3.6, 3.5 and 3.8, and the value of CV was 6.2 (*middle* and *right*)

of about 30% in the total lesion volume was shown [21]. As respiratory motion resulted in the spread of the tumor contour to a larger size than the correct outline, the value of MV seemed to be overestimated. Although the clinical significance of the MV had not been determined yet, the index was also likely to reflect the exact viable tumor tissue amount [22]. The values of MV positively correlated well with those of SUV_{max} in our previous study and the coefficient correlations were around 0.6–0.7 [22]. The value of MV would also preferably be calculated by the DIBH technique.

With regard to the reproducibility of DIBH, the mean value of CV in calculating SUV_{max} was fairly good, at around 5–6. In calculating MV, the CV value was 7.1 in thoracic lesions and 11.9 in abdominal lesions. These were better than those of phantom studies with low-dose condition. Although the value of CV was higher than that obtained in the phantoms with middle-dose or high-dose conditions, they would be acceptable values clinically if we recognize the ranges of values. Interestingly, the mean values of CV of both indices were better in thoracic lesions compared with those in abdominal lesions. A possible explanation regarding the relatively higher CV of the abdominal lesions may be that larger attenuation correction factors including surrounding physiological uptake are applied in this section compared to the thorax (lower attenuation due to the lungs). Such a difference in anatomical and physiological conditions was considered to be the main influencing factor.

The other possible influential factor is the length of acquisition time with breath holding. We set 30 s for each datum in each study to gather adequate counts for maintaining image qualities and reproducibility. Although the value of CV in 30-s collection is known to be better than that in 15-s collection in phantom study [16], 30-s breath holding might be difficult in some cases. In some previous studies on DIBH protocols, various and flexible breath-holding times using list mode collections were set [16].

Table 3 Comparison of quantitative indices (clinical studies)

	Thoracic lesions ($n = 28$)	Abdominal lesions ($n = 47$)
SUV_{max}		
NBH	9.1 ± 7.5	9.5 ± 4.4
DIBH	12.0 ± 8.9*	13.5 ± 7.3*
CV	5.5 ± 2.9	6.3 ± 4.8
MV (cm^3)		
NBH	25.7 ± 19.4	24.3 ± 17.9
DIBH	21.6 ± 18.3*	20.4 ± 15.9**
CV	7.1 ± 6.7	11.9 ± 8.6
Maximal diameter (mm)	28.8 ± 14.8	36.3 ± 15.5

NBH Non-breath hold

DIBH Deep-inspiration breath hold

The maximal diameter was calculated as the mean value of lesions

* $P < 0.01$; the value of DIBH was significantly higher than that of NBH

** $P < 0.05$; the value of DIBH was significantly lower than that of NBH

Even in patients with respiratory dysfunction, DIBH data acquisition is possible under an optimal condition by the list mode collections. In contrast, we fixed the length of each breath-holding time at 30 s. Although we made the series of examination uniform and could promote the efficiency of DIBH studies, subtle difference within 4 DIBH studies might account for the higher CV values.

Another probable influential factor is the tumor component. Because we selected only tumors with a solid component, lesion homogeneity was assured equally in each study. In cases with inhomogeneous tumors, such as cavity forming ones or ones containing a cystic component, the reproducibility would be worse.

Taking into account the result that the values of SUV_{max} of a lesion with DIBH technique were higher than those with NBH PET/CT, the optimal threshold of SUV_{max} for differentiating between benign and malignant tumors should be re-evaluated under well-controlled respiratory motion. The criteria of the value of the SUV-related index, such as the percentage of increase of a dual-phase study or MV, in differentiation or staging should also be evaluated in the future.

The other implication is the contribution of this technique to the strategy for cancer treatment [14, 23]. Recently, radiotherapy has become more effective in various tumors [23, 24]. As accurate tumor location is an important factor for determining the therapeutic method, correct diagnosis using the DIBH technique for anatomical assignment is important [25]. When MV is used as a guide for the radiotherapy planning target volume, a greater dose to the normal tissues may be irradiated under the NBH condition. This kind of unnecessary overdose could be avoided by the DIBH technique.

Although the DIBH technique has a drawback in clinical use, that is, limited availability within only a one-bed range at present, it will become a standard method if the sensitivity of the PET/CT system is improved further and the longitudinal fields of view are increased. Future studies should be done under an optimal protocol and appropriate data collection time in multiple institutions.

Conclusion

The DIBH ^{18}F-FDG PET/CT corrects the inaccurate quantification of both SUV_{max} and MV. The reproducibility of calculation in SUV_{max} or MV with DIBH technique is favorable. However, at present it is better applicable to thoracic than abdominal lesions.

References

1. Kim SK, Allen-Auerbach M, Goldin J, Fueger BJ, Dahlbom M, Brown M, et al. Accuracy of PET/CT in characterization of solitary pulmonary lesions. J Nucl Med. 2007;48:214–20.
2. Halpern BS, Yeom K, Fueger BJ, Lufkin RB, Czernin J, Allen-Auerbach M. Evaluation of suspected local recurrence in head and neck cancer: a comparison between PET and PET/CT for biopsy-proven lesions. Eur J Radiol. 2007;62:199–204.
3. Mottaghy FM, Sunderkötter C, Schubert R, Wohlfart P, Blumstein NM, Neumaier B, et al. Direct comparison of [18F] FDG PET/CT with PET alone and with side-by-side PET and CT in patients with malignant melanoma. Eur J Nucl Med Mol Imaging. 2007;34:1355–64.
4. Nehmeh SA, Erdi YE. Respiratory motion in positron emission tomography/computed tomography: a review. Semin Nucl Med. 2008;38:167–76.
5. Cohade C, Osman M, Marshall LN, Wahl RN. PET-CT: accuracy of PET and CT spatial registration of lung lesions. Eur J Nucl Med Imaging. 2003;30:721–6.
6. Francis DL, Visvikis D, Costa DC, Arulampalam TH, Townsend C, Luthra SK, et al. Potential impact of [18F] 3′-deoxy-3′-fluorothymidine versus [18F]fluoro-2-deoxy-D-glucose in positron emission tomography for colorectal cancer. Eur J Nucl Med Imaging. 2003;30:344–53.
7. Dawood M, Lang N, Jiang X, Schäfers KP. Lung motion correction on respiratory gated 3-D PET/CT images. IEEE Trans Med Imaging. 2006;25:476–85.
8. Townsend DW. Dual-modality imaging: combining anatomy and function. J Nucl Med. 2008;49:938–55.
9. Vogel WV, van Dalen JA, Wiering B, Huisman H, Corstens FH, Ruers TJ, et al. Evaluation of image registration in PET/CT of the liver and recommendations for optimized imaging. J Nucl Med. 2007;48:910–9.
10. Larson SM, Nehmeh SA, Erdi YE, Humm JL. PET/CT in non-small-cell lung cancer: value of respiratory-gated PET. Chang Gung Med J. 2005;28:306–14.
11. Boucher L, Rodrigue S, Lecomte R, Bénard F. Respiratory gating for 3-dimensional PET of the thorax: feasibility and initial results. J Nucl Med. 2004;45:214–9.

12. Hamill JJ, Bosmans G, Dekker A. Respiratory-gated CT as a tool for the simulation of breathing artifacts in PET and PET/CT. Med Phys. 2008;35:576–85.
13. Daouk J, Fin L, Bailly P, Meyer ME. Respiratory-gated positron emission tomography and breath-hold computed tomography coupling to reduce the influence of respiratory motion: methodology and feasibility. Acta Radiol. 2009;50:144–55.
14. Meirelles GSP, Erdi YE, Nehmeh SA, Squire OD, Larson SM, Humm JL, et al. Deep-inspiration breath-hold PET/CT: clinical findings with a new technique for detection and characterization of thoracic lesions. J Nucl Med. 2007;48:712–9.
15. Nehmeh SA, Erdi YE, Meirelles GSP, Squire O, Larson SM, Humm JL, et al. Deep-inspiration breath-hold PET/CT of the thorax. J Nucl Med. 2007;48:22–6.
16. Kawano T, Ohtake E, Inoue T. Deep-inspiration breath-hold PET/CT of lung cancer: maximum standardized uptake value analysis of 108 patients. J Nucl Med. 2008;49:1223–31.
17. Yamaguchi T, Ueda O, Hara H, Sakai H, Kida T, Suzuki K, et al. Usefulness of a breath-holding acquisition method in PET/CT for pulmonary lesions. Ann Nucl Med. 2009;23:65–71.
18. Erdi YE, Nehmeh SA, Pan T, Pevsner A, Rosenzweig KE, Mageras G, et al. The CT motion quantitation of lung lesions and its impact on PET-measured SUVs. J Nucl Med. 2004;45:1287–92.
19. Nehmeh SA, Erdi YE, Ling CC, Rosenzweig KE, Schoder H, Larson SM, et al. Effect of respiratory gating on quantifying PET images of lung cancer. J Nucl Med. 2002;43:876–81.
20. Nehmeh SA, Erdi YE, Pan T, Pevsner A, Rosenzweig KE, Yorke E, et al. Four-dimensional (4D) PET/CT imaging of the thorax. Med Phys. 2004;31:3179–86.
21. Nehmeh SA, Erdi YE, Ling CC, Rosenzweig KE, Squire OD, Braban LE, et al. Effect of respiratory gating on reducing lung motion artifacts in PET imaging of lung cancer. Med Phys. 2002;29:366–71.
22. Kiyohara S, Nagamachi S, Wakamatsu H, Fujita S, Nishii R, Kamimura M, et al. The usefulness of metabolic volume in diagnosing malignant tumor in FDG-PET/CT. Jpn J Clin Radiol. 2008;53:997–1003.
23. Zeng ZC, Tang ZY, Fan J, Zhou J, Qin LX, Ye SL, et al. Consideration of the role of radiotherapy for unresectable intrahepatic cholangiocarcinoma: a retrospective analysis of 75 patients. Cancer J. 2006;12:113–22.
24. Ben-David MA, Griffith KA, Abu-Isa E, Lawrence TS, Knol J, Zalupski M, et al. External-beam radiotherapy for localized extrahepatic cholangiocarcinoma. Int J Radiat Oncol Biol Phys. 2006;66:772–9.
25. Takeuchi S, Saito H, Hokodate H, Yuasa N, Takei T, Takamura A. Criteria for Indications for IVR Therapy from the standpoint of MDCT, MRI and Technical Points. Jpn J Diagn Imaging. 2006;26:585–94.